J Nanopart Res
DOI 10.1007/s11051-009-9611-4

RESEARCH PAPER

# Nanosized cancer cell-targeted polymeric immunomicelles loaded with superparamagnetic iron oxide nanoparticles

**Rishikesh M. Sawant · Rupa R. Sawant · Evin Gultepe · Dattatri Nagesha · Brigitte Papahadjopoulos-Sternberg · Srinivas Sridhar · Vladimir P. Torchilin**

Received: 26 October 2008 / Accepted: 17 February 2009


**Abstract** Stable 30–50 nm polymeric polyethylene glycol–phosphatidylethanolamine (PEG–PE)-based micelles entrapping superparamagnetic iron oxide nanoparticles (SPION) have been prepared. At similar concentrations of SPION, the SPION-micelles had significantly better magnetic resonance imaging (MRI) T2 relaxation signal compared to 'plain' SPION. Freeze-fracture electron microscopy confirmed SPION entrapment in the lipid core of the PEG–PE micelles. To enhance the targeting capability of these micelles, their surface was modified with the cancer cell-specific anti-nucleosome monoclonal antibody 2C5 (mAb 2C5). Such mAb 2C5-SPION immunomicelles demonstrated specific binding with cancer cells in vitro and were able to bring more SPION to the cancer cells thus demonstrating the potential to be used as targeted MRI contrast agents for tumor imaging.

**Keywords** Superparamagnetic iron oxide nanoparticles · Polymeric micelles · Immunomicelles · Cancer-specific monoclonal antibody · MRI contrast agent · Nanomedicine

R. M. Sawant · R. R. Sawant · V. P. Torchilin (✉)
Department of Pharmaceutical Sciences, Center for Pharmaceutical Biotechnology and Nanomedicine, Northeastern University, Mugar Building, Room 312, 360 Huntington Avenue, Boston, MA 02115, USA
e-mail: v.torchilin@neu.edu

E. Gultepe · D. Nagesha · S. Sridhar
Electronic Materials Research Institute, Northeastern University, Boston, MA 02115, USA

B. Papahadjopoulos-Sternberg
Nano Analytical Laboratory, 3951 Sacramento Street, San Francisco, CA 94118, USA

## Introduction

Superparamagnetic iron oxide nanoparticles (SPION) have received increased attention due to their characteristic small size (4–10 nm) and magnetic properties. SPION exist mostly either as magnetite ($Fe_3O_4$) or maghemite ($\gamma$-$Fe_2O_3$). As the name suggests, these nanoparticles exhibit paramagnetism, i.e., they acquire large magnetic moments in the presence of external magnetic field and lose magnetic properties upon the removal of this field (Gupta and Gupta 2005; Corot et al. 2006). It is because of this property, there was a significant interest in developing SPION for their application as MRI contrast agents (Kang et al. 2002; Durand et al. 2007; Mulder et al. 2007; Sun et al. 2008) as well as for live cell tracking (Sykova and Jendelova 2007), magnetic targeting (Alexiou et al. 2003; Dandamudi and Campbell 2007; Martina et al. 2007; Mathieu and Martel 2007; Silva et al. 2007; Tang et al. 2007; Zhang et al. 2007; Yang et al. 2008), alternating

Published online: 08 March 2009

current (AC)-assisted hyperthermia anti-cancer (Ito et al. 2006; Johannsen et al. 2006; Fortin et al. 2007; Jin et al. 2008), and many other applications [for reviews refer (Gupta and Gupta 2005; Ito et al. 2005; Corot et al. 2006; Silva et al. 2007)].

However, 'plain' SPION are not stable at normal physiological conditions and show a tendency to aggregate because of their high hydrophobic nature and small size. They often need to be coated with different polymers in order to stabilize them in suspension. Attempts have been made to stabilize SPION by their incorporation into liposomes (Kubo et al. 2001; Dandamudi and Campbell 2007), polymeric micelles (Ai et al. 2005; Nasongkla et al. 2006), microemulsions (Munshi et al. 1997) as well as by their surface coating with dextran (Wada et al. 2003) and many other polymers. High accumulation of SPION in target organs is a usual requirement for better MRI contrast and/or AC-assisted hyperthermic anti-cancer therapy. Still, even stabilized SPION when administered parenterally, distribute into tissues and organs non-specifically, with no specific accumulation into areas of interest.

Polyethylene glycol–phosphatidylethanolamine (PEG–PE)-based polymeric micelles have been proven to be the delivery system of choice for various hydrophobic drugs/diagnostic agents, since they demonstrate a prolonged blood circulation and can be functionalized through PEG water-exposed termini with various target-specific ligands. In our previous work, we have shown that the micelles prepared from PEG–PE conjugates can be efficiently loaded with various poor water-soluble anti-cancer drugs and they accumulate into experimental tumors via the enhanced permeability and retention (EPR) effect (Torchilin 2004). In addition, these micelles can also be decorated with various specific ligands attached to their outer surface (distal termini of PEG chains). Thus, the anti-cancer nucleosome-specific monoclonal antibody 2C5 (mAb 2C5) was attached to such micelles, which recognizes the surface of a broad variety of tumor cells (but not normal cells) via tumor cell surface-bound nucleosomes (Iakoubov et al. 1995; Iakoubov and Torchilin 1997, 1998; Torchilin et al. 2004), making the resulting immunomicelles capable of specifically targeting a broad variety of tumors (Torchilin et al. 2003; Elbayoumi et al. 2007; Sawant et al. 2008). In these studies, it was also clearly demonstrated that mAb 2C5-modified pharmaceutical nanocarriers demonstrate high specificity toward cancer cells showing very little if at all uptake by normal cells, and internalizable mAb 2C5 enhances the internalization of drug-loaded nanocarriers by cancer cells (Torchilin et al. 2003; Lukyanov et al. 2004; Gupta et al. 2005).

Here, we attempted to combine the longevity of PEG–PE polymeric micelles and their targetability by the mAb 2C5 to produce SPION-loaded mAb 2C5-PEG–PE polymeric immunomicelles capable of bringing an increased quantity of SPION to cancer cells for various therapeutic and diagnostic applications including MRI.

## Experimental

### Materials

1,2-Distearoyl-*sn*-glycero-3-phosphoethanolamine-*N*-[poly(ethyleneglycol)2000] ($PEG_{2000}$–PE) and 1,2-dipalmitoyl-*sn*-glycero-3-phosphoethanolamine-*N*-[lissamine rhodamine B sulfonyl] [ammonium salt] (Rhodamine–PE or Rh–PE) were purchased from Avanti Polar Lipids (Alabaster, AL, USA). Trimethylamine oxide [$(CH_3)_3NO$], Iron(0) pentacarbonyl [$Fe(CO)_5$], hexane, ethanol, octyl ether, and all other chemicals were purchased from Sigma Chem., Inc. (St. Louis, MO, USA). HOECHST 33342 was purchased from Invitrogen Corp. (Carlsbad, CA, USA). Dulbecco's Modified Eagle's Medium, Hanks' Balanced Salt Solution (HBSS), fetal bovine serum, and penicillin/streptomycin stock solutions were purchased from CellGro (Kansas City, MO, USA). Tissue culture grade fetal bovine serum and trypsin were obtained from ICN Biomedicals (Costa Nesa, CA, USA). The production and purification of the anti-nucleosomal cancer-specific mAb 2C5 were carried out by Harlan Bioproducts (Indianapolis, IL, USA) using the hybridoma cell line from our laboratory. Control bovine IgG antibody was purchased from Millipore Corp. (Bedford, MA, USA). p-Nitrophenylcarbonyl-polyethyleneglycol-3400-phosphatidylethanolamine (pNP–$PEG_{3400}$–PE) was synthesized in our lab according to the procedure described earlier (Torchilin et al. 2001). Cancer cell lines were purchased from the American Type Culture Collection (Rockville, MD, USA). Distilled and deionized water was used in all experiments.

## Synthesis of SPION

The nanoparticles were synthesized using the thermal decomposition method developed by Hyeon et al. with some slight modifications (Hyeon et al. 2001). In brief, 1.28 g oleic acid was dissolved in 10 mL octyl ether, and then heated to about 100 °C. To this solution, 200 μL of $Fe(CO)_5$ was added. The mixture was refluxed at 280 °C for 1 h and then cooled to room temperature. The solution changed color from pale-yellow green to dark black during the heating process. To this mixture 0.34 g of $(CH_3)_3NO$ was added along with 500 μL of octyl ether to facilitate complete transfer of the salt. The mixture was then heated to 130 °C for 2 h under argon atmosphere. The temperature was slowly increased to reflux temperature of 280 °C and maintained for an additional 1 h. The iron oxide nanoparticles were precipitated out from this solution using ethanol, separated from the supernatant by centrifugation, dried under argon, weighed, and re-dispersed in hexane to obtain a 1.5 mg/mL SPION solution. SPION obtained by this method were typically in the range of 4–6 nm as determined by transmission electron microscopy (data not shown).

## Preparation of SPION-micelles

SPION-micelles were prepared by the lipid film rehydration method. Briefly, 10 mg of $PEG_{2000}$–PE in chloroform and 0.25 mg of SPION in hexane were mixed and the organic solvents were removed by rotary evaporator. Any residual solvents were removed by using freeze-dryer overnight. The dry film was than rehydrated using 2 mL 10 mM HEPES-buffered saline (HBS) pH 7.4 by vortexing for 5 min followed by the bath sonication for 5 min to get SPION-loaded PEG–PE micelles. Since the transition temperature of PEG–DSPE is above 37 °C, we have performed the sonication at room temperature with cooling to keep the system below the transition temperature. The micelle size was determined by the dynamic light scattering (DLS) in ZetaPlus particle size analyzer (Brookhaven Instruments Corporation Holtsville, NY, USA).

## Freeze-fracture electron microscopy

For determining the structure of the micelles after the incorporation of SPION, the freeze-fracture electron microscopy was carried out for 'plain' PEG–PE micelles and SPION-micelles (10 mg/mL in HBS pH 7.4). The sample was quenched by using the sandwich technique and liquid nitrogen-cooled propane. A cooling rate of 10,000 K $s^{-1}$ avoids ice crystal formation and artifacts possibly caused by the cryofixation process. The cryo-fixed samples were stored in liquid nitrogen for <2 h before processing. The fracturing process was carried out in JEOL JED-9000 freeze-etching equipment, and the exposed fracture planes were shadowed with platinum for 30 s at an angle of 25–35° and with carbon for 35 s (2 kV, 60–70 mA, $1 \times 10^{-5}$ torr). The replicas were cleaned with fuming $HNO_3$ for 24 h followed by repeated agitation with fresh chloroform/methanol (1:1 by vol) at least five times and examined with a JEOL 100 CX electron microscope.

## Magnetic resonance relaxation rate of 'plain' SPION and SPION-micelles

When used as contrast agent for MRI, SPION increase the relaxation rate of water and have the greatest effect on the T2 (spin–spin) relaxation rate. However, this change in the relaxation rate depends on the size of the SPION, degree of aggregation, surface coating thickness, etc. In vitro relaxation parameters of both the 'plain' SPION (i.e. SPION dispersed in HBS, pH 7.4) and SPION-micelle samples were measured using a benchtop 5 mHz RADX NMR Proton Spin Analyzer at room temperature in HBS, pH 7.4, at different SPION concentrations.

## Preparation of SPION-immunomicelles

First, mAb 2C5 or nonspecific control bovine IgG was conjugated to pNP–$PEG_{3400}$–PE as previously with some modifications (Lukyanov et al. 2004; Elbayoumi et al. 2007; Elbayoumi et al. 2007; Elbayoumi and Torchilin 2008). In brief, 14 mg $PEG_{2000}$–PE (97 mol.%), 0.45 mg pNP–$PEG_{3400}$–PE (2 mol.%), 0.064 mg Rh-PE (1 mol.%) in chloroform and 0.35 mg SPION in hexane were dried in a rotary evaporator and freeze-dryer to form a thin film. The film was hydrated with 1 mL of 5 mM citrate buffered saline, pH 5.0, by vortexing for 5 min followed by bath sonication for 5 min to form the micelle solution. Separately, 1 mL solution (1.56 mg/mL)

of the mAb 2C5 or non-specific bovine gamma immunoglobulin antibody (IgG) was prepared in 50 mM phosphate-buffered saline, pH 8.7, and incubated with the above micelle solution with stirring overnight at 4 °C to allow the attachment of the antibody to the activated PEG terminus with the simultaneous hydrolysis of non-reacted pNP groups, thus forming the SPION-2C5-immunomicelles. The formulations were then purified using dialysis bags MWCO 250 kDa against HBS, pH 7.4, with four changes within 6 h. After purification, the antibody concentration in the micelle preparation was estimated by the BCA protein assay kit (Pierce Biotechnology, Inc. Rockford, IL, USA) according to manufacturer's recommendations. The micelle size was confirmed by DLS in ZetaPlus particle size analyzer (Brookhaven Instruments Corporation Holtsville, NY, USA).

### ELISA of immunomicelles

The specific activity of the immunomicelles was determined by ELISA as described below. An ELISA assay (indirect, using an enzyme-tagged secondary Ab) was performed to show the ability of the SPION-immunomicelles to recognize the target antigen, nucleosomes (NS). The 96-well plates were coated with 50 μL of 40 μg/mL poly-L-lysine (MW 30–70 kDa). After discarding the poly-L-lysine solution, the wells were blocked with 200 μL of TBS containing 0.05% w/v Tween 20 and 2 mg/mL casein (TBST-casein) for 1 h at RT, and then incubated with 50 μL of 40 μg/mL NS in TBST-casein for 1 h at RT and washed three times with TBST. Then, the wells were incubated with different concentrations of the native mAb 2C5 and mAb2C5- and IgG-modified SPION immunomicelles for 1 h at RT. After the incubation, the wells were washed as before and incubated with 50 μL/well of 1:5000 dilution of goat anti-mouse IgG peroxidase conjugate (ICN Biomedicals, Inc., Aurora, OH) in TBST-casein for 1 h at RT. The wells were again washed as before, and each well was incubated with 100 μL of enhanced Kblue TMB peroxidase substrate (Neogen Corporation, Lexington, KY) for 15 min. The microplate was read at a dual wavelength of 620 nm with the reference filter at 492 nm using a Labsystems Multiskan MCC/340 microplate reader installed with GENESISLITE windows-based microplate software.

### Cell culture

Human breast carcinoma MCF-7 (American Type Culture Collection, Manassas, VA, USA) cells were maintained in DMEM cell culture medium at 37 °C, 5% $CO_2$. DMEM media were supplemented with 10% fetal bovine serum, 1 mM Na-pyruvate, 50 U/mL penicillin, and 50 μg/mL streptomycin.

### Interaction of SPION-loaded mAb 2C5-immunomicelles with cancer cells in vitro

After the initial passage in tissue culture flasks, MCF-7 cells were grown on coverslips in 6-well tissue culture plates (100,000 cells per well) in DMEM with 10% BSA. After the cells reached a confluence of 70–80%, the plates were washed and blocked with 1% BSA in DMEM. Rhodamine–PE (Rh–PE)-labeled micelle samples in a serum-free medium were added to the cells at a final PEG–PE concentration of 0.35–0.70 mM and incubated for 2 h at 37 °C, 5% $CO_2$. After the incubation, the cells were washed using three 1 mL washes of HBSS. The cells were then digested using trypsin and collected in HBSS. T2 relaxation times for the cell samples were measured using Varian INOVA 500 MHz NMR spectrometer at room temperature in HBSS. The rhodamine fluorescence associated with the cells was also measured using the Hitachi L2000 fluorospectrometer at the excitation wavelength of 550 nm and emission wavelength of 590 nm.

### Fluorescence microscopy

After the initial passage in tissue culture flasks, MCF-7 cells were grown on coverslips in 6-well tissue culture plates (50,000 cells per well) in DMEM with 10% BSA. After the cells reached a confluence of 40–50%, the plates were washed and blocked with 1% BSA in DMEM. Rh–PE-labeled micelle samples in serum-free medium were added to the cells at a final PEG–PE concentration of 0.35–0.70 mM and incubated for 2 h at 37 °C, 5% $CO_2$. After the incubation, the cells were washed using three 1 mL washes of HBSS. The cells were stained with HOECHST 33342 at 5 μg/mL for 3 min followed by washing with HBSS. Individual coverslips were mounted cell-side down onto fresh glass slides with PBS. Cells were viewed and pictures were taken with

a Nikon Eclipse E400 microscope using the epifluorescence microscopy.

## Results and discussion

### Size and size distribution of SPION-micelles

SPION-micelles were prepared in HBS, pH 7.4, by the lipid film rehydration method. The formulations were found to be stable with the size ranging from 25 to 50 nm as determined by DLS (Fig. 1). No significant change in size was observed after the formulations were kept at room temperature for over 2 weeks (data not shown). On the other hand, the 'plain' SPION by themselves could not be suspended in HBS, pH 7.4, thus showing a visible aggregation.

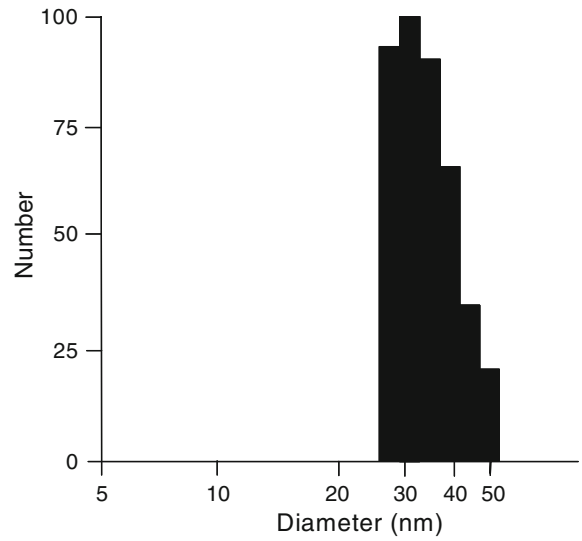


**Fig. 1** Typical size distribution of SPION-micelles suspended in HBS, pH 7.4

### Freeze-fracture electron microscopy

Freeze-fracture electron microscopy was used to study the morphology of the SPION-micelles and confirms whether there is a difference from the morphology of 'plain' PEG–PE micelles as well as for determining whether the SPION were loaded inside the lipid core of the PEG–PE micelles or were present as aggregates externally. As could be clearly seen from the electron micrographs taken from several freeze-fracture preparations of either 'plain' PEG–PE micelles or SPION-loaded PEG–PE micelles, both samples contain medium concentration of small (ca. 30–50 nm), overall spherical particles, which indicated that the normal morphology of the micelles was maintained. They display their shadows behind the structure, which is typical for 'tight-core' particles such as micelles. The only clear difference in electron micrographs of the two samples was that in case of SPION-loaded PEG–PE micelles, the structures show, in addition, a darker inner core, which is a clear indication of encapsulated SPION (for typical micrographs, see Fig. 2).

### Magnetic resonance relaxation rate of 'plain' SPION and SPION-micelles

For any MRI contrast, the relaxation rate depends on the size of the contrast agent, degree of aggregation, and concentration. PEG–PE-based polymeric micelles were able to prevent the SPION form

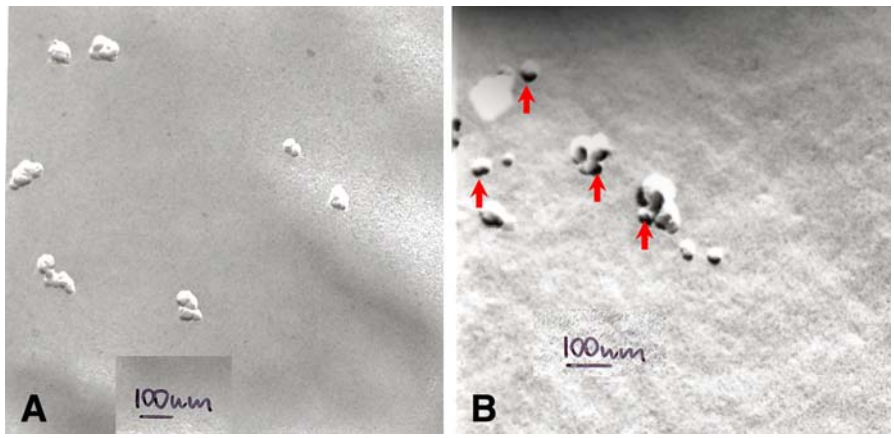


**Fig. 2** Freeze-fracture micrographs of **a** 'plain' PEG–PE micelles and **b** SPION-loaded PEG–PE micelles (*red* arrows pointing at darker inner core)

aggregation, and hence the T2 relaxation rate was much greater in the case of SPION-micelles when compared to 'plain' SPION at same concentration (see Fig. 3). For example, at the concentration of 0.0625 mg/mL of SPION, the relaxation rate of SPION-micelles was more than 30 times the relaxation rate of 'plain' SPION. This is a very important and desirable property for developing MRI contrast agents as more intense MRI signals will be obtained at low concentrations of SPION, thus preventing unnecessary high dose of the contrast agent to get clinically relevant MRI images of the pathological organs.

## SPION-immunomicelles and their characterization

In order to further improve the SPION-micelles, we modified their outer PEG corona with tumor cell-targeting nucleosome-specific mAb 2C5, using a simple and reproducible chemistry using pNP–$PEG_{3400}$–PE (Torchilin et al. 2001). As was seen previously, in the attachment of mAb 2C5, there was almost no change in size of the SPION-immunomicelles. SPION-immunomicelles were fluorescently labeled using Rh–PE to follow their interaction with cells in vitro. The conjugation of the antibody to the Rh–PE-labeled SPION-micelles was gentle enough, as follows from the ELISA assay, and the activity of the mAb 2C5-SPION-immunomicelles toward the specific antigen, nucleosomes, was maintained almost at the level of native unmodified mAb 2C5. The 'plain' SPION-micelles or non-specific bovine IgG-modified SPION-micelles did not show any binding to the monolayer of the nucleosomal antigen (Fig. 4).

## In vitro cell interaction of mAb 2C5 SPION-immunomicelles

After ensuring that the mAb 2C5 maintained its specific activity upon the conjugation to SPION-micelles (2C5-SPION-micelles), their interaction with human breast tumor cell line MCF-7 in vitro was carried out using both epifluorescence microscopy and fluorescence spectrometer using bovine IgG SPION-micelles and "Plain" SPION-micelles as control.

After incubating the SPION-micelle formulations with the cells, any free unbound micelle is removed during the HBSS washing. As can be seen in epifluorescence microscopy pictures in Fig. 5, the specificity of the conjugated mAb 2C5 resulted in the increased association of these micelles with the MCF-7 cells, when cells were incubated with mAb 2C5-SPION-immunomicelles in comparison to the 'plain' and 'non-specific' bovine IgG-modified SPION-micelles (following the micelle-associated Rh fluorescence). One has to notice here that the lack of any specific interaction of mAb 2C5-modified pharmaceutical nanocarriers with normal cells was repeatedly shown in many of our previous

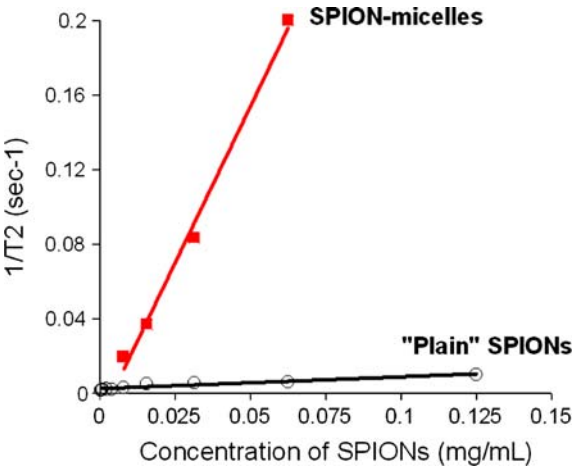


**Fig. 3** In vitro relaxation rate comparison of 'plain' SPION and SPION-micelles at different concentrations of SPIONs

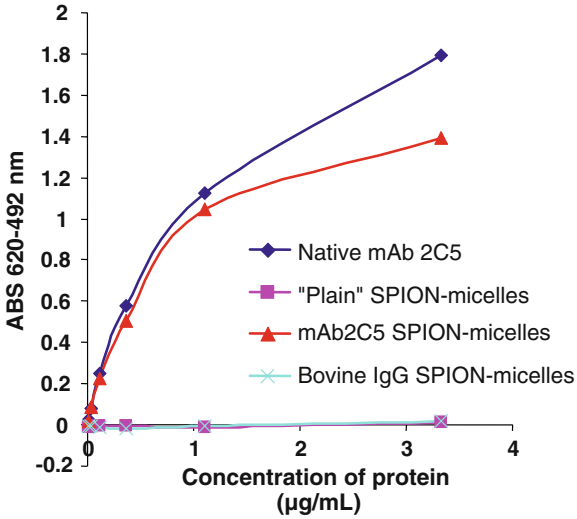


**Fig. 4** Binding of mAb 2C5 SPION-immunomicelles and control 'plain' SPION-micelles or bovine IgG SPION-micelles to a monolayer of nucleosomes

experiments (Iakoubov et al. 1995, Torchilin et al. 2003; Elbayoumi and Torchilin 2007; Erdogan et al. 2008).

In order to quantify the amount of fluorescence associated with the cells, the cells were digested/lysed using trypsin and the cell lysate fluorescence was measured using fluorescence spectrometer. In agreement to the epifluorescence microscopy results, the fluorescence associated with MCF-7 cells was significantly higher in case of cells treated with mAb 2C5-SPION-micelles in comparison to the 'plain' and 'non-specific' bovine IgG-modified SPION-micelles (Fig. 6).

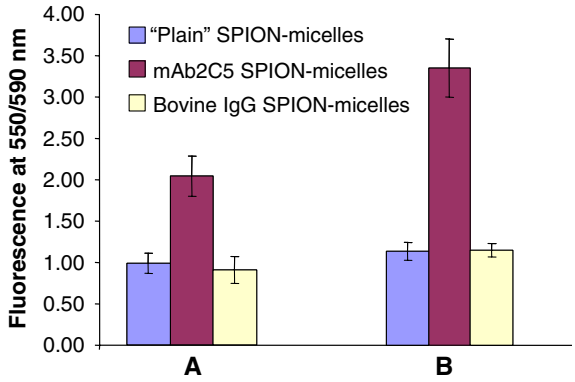


**Fig. 6** Cell-associated rhodamine fluorescence using fluorescence spectrometer using micelles at concentration of (a) 0.35 mM PEG–PE or (b) 0.70 mM PEG–PE

## T2 relaxation rates of mAb2C5 SPION-immunomicelles on cells in vitro

The aim of developing cancer cell-targeted SPION-micelles was to ensure that the higher amount of SPION is carried to the cancer cells for their more efficient magnetic resonance imaging. We determined the T2 relaxation time of the lysed cells after their co-incubation with plain, non-specific IgG-modified or mAb 2C5-modified SPION-micelles. The signal associated with the cells was determined using 500 MHz NMR. As expected, we observed a significant increase in cell-associated T2 relaxation rate (1/T2) in case of cells treated with mAb 2C5 SPION-immunomicelles (compared with the treatment with non-targeted SPION-micelles) as seen in the Table 1. This increased signal is the direct result of target cell recognition by mAb 2C5-SPION-immunomicelles.

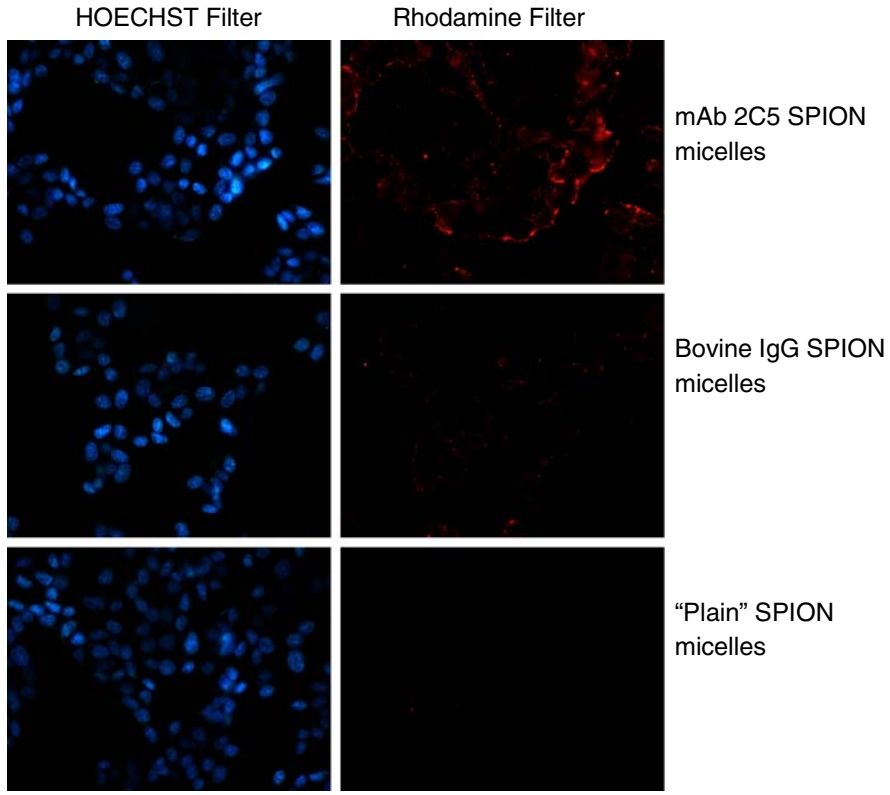


**Fig. 5** Increased fluorescence can be observed from epifluorescence microscopy of human breast cancer MCF-7 cells after incubation with SPION-micelles for 2 h. *Left panel* shows nuclear HOECHST 33342 staining of the cell nuclei and the *right panel* shows associated micellar rhodamine fluorescence from the micelles. Magnification of images at 40× objective

**Table 1** Relaxivity R2 (1/T2) of the MCF-7 cells after the incubation with different concentrations of micellar preparations

| Formulations | Concentration of PEG–PE applied to MCF-7 cells. | |
|---|---|---|
| | 0.35 mM | 0.70 mM |
| 'Plain' SPION-micelles | $4.3 \pm 0.02\ s^{-1}$ | $5.2 \pm 0.05\ s^{-1}$ |
| mAb 2C5 SPION-micelles | $5.6 \pm 0.01\ s^{-1}$ | $7.1 \pm 0.02\ s^{-1}$ |
| Bovine IgG SPION-micelles | $4.3 \pm 0.00\ s^{-1}$ | $6.0 \pm 0.02\ s^{-1}$ |

The relaxivity of the sample increases when larger quantity of SPION is associated with the cells

## Conclusion

PEG–PE-based polymeric micelles offer a convenient carrier system for suspending SPION in aqueous medium. The formulations were stable with no apparent aggregation compared to that observed in the case of 'plain' SPION. SPION-loaded PEG–PE micelles provided dramatically improved T2 relaxation rates. These SPION-micelles can be easily modified with anti-cancer nucleosome-specific mAb 2C5 with the preservation of the antibody specific activity to make them cancer cell-specific. mAb 2C5-SPION-immunomicelles specifically recognize and bind cancer cells in vitro, bring higher quantity of SPION to these cells, and have a potential to serve as an MRI contrast agent with improved T2 for better tumor imaging. In addition to this, the specific accumulation of mAb 2C5-SPION-immunomicelles into the cancer cells makes these micelles good candidates to be used in conjunction with AC-field-assisted hyperthermic cancer therapy.

**Acknowledgment** This work was supported by the NIH grants RO1 EB01961 and RO1 EN002995 to Vladimir P. Torchilin and by Northeastern University and NSF grant DGE-0504331 to Srinivas Sridhar.

## References

Ai H, Flask C, Weinberg B, Shuai X, Pagel MD, Farell D, Duerk J, Gao J (2005) Magnetite-loaded polymeric micelles as novel magnetic resonance probes. Adv Mater 26: 3995–4021

Alexiou C, Jurgons R, Schmid RJ, Bergemann C, Henke J, Erhardt W, Huenges E, Parak F (2003) Magnetic drug targeting-biodistribution of the magnetic carrier and the chemotherapeutic agent mitoxantrone after locoregional cancer treatment. J Drug Target 11:139–149. doi:10.1080/1061186031000150791

Corot C, Robert P, Idee JM, Port M (2006) Recent advances in iron oxide nanocrystal technology for medical imaging. Adv Drug Deliv Rev 58:1471–1504. doi:10.1016/j.addr.2006.09.013

Dandamudi S, Campbell RB (2007) Development and characterization of magnetic cationic liposomes for targeting tumor microvasculature. Biochim Biophys Acta 1768:427–438. doi:10.1016/j.bbamem.2006.10.006

Durand E, Raynaud JS, Bruneval P, Brigger I, Al Haj Zen A, Mandet C, Lancelot E, Lafont A (2007) Magnetic resonance imaging of ruptured plaques in the rabbit with ultrasmall superparamagnetic particles of iron oxide. J Vasc Res 44:119–128. doi:10.1159/000098484

Elbayoumi TA, Torchilin VP (2007) Enhanced cytotoxicity of monoclonal anticancer antibody 2C5-modified doxorubicin-loaded PEGylated liposomes against various tumor cell lines. Eur J Pharm Sci 32:159–168. doi:10.1016/j.ejps.2007.05.113

Elbayoumi TA, Torchilin VP (2008) Tumor-specific antibody-mediated targeted delivery of Doxil® reduces the manifestation of auricular erythema side effect in mice. Int J Pharm 357:272–279. doi:10.1016/j.ijpharm.2008.01.041

Elbayoumi TA, Pabba S, Roby A, Torchilin VP (2007) Anti-nucleosome antibody-modified liposomes and lipid-core micelles for tumor-targeted delivery of therapeutic and diagnostic agents. J Liposome Res 17:1–14. doi:10.1080/08982100601186474

Erdogan S, Medarova ZO, Roby A, Moore A, Torchilin VP (2008) Enhanced tumor MR imaging with gadolinium-loaded polychelating polymer-containing tumor-targeted liposomes. J Magn Reson Imaging 27:574–580. doi:10.1002/jmri.21202

Fortin JP, Wilhelm C, Servais J, Menager C, Bacri JC, Gazeau F (2007) Size-sorted anionic iron oxide nanomagnets as colloidal mediators for magnetic hyperthermia. J Am Chem Soc 129:2628–2635. doi:10.1021/ja067457e

Gupta AK, Gupta M (2005) Synthesis and surface engineering of iron oxide nanoparticles for biomedical applications. Biomaterials 26:3995–4021. doi:10.1016/j.biomaterials.2004.10.012

Gupta B, Levchenko TS, Mongayt DA, Torchilin VP (2005) Monoclonal antibody 2C5-mediated binding of liposomes to brain tumor cells in vitro and in subcutaneous tumor model in vivo. J Drug Target 13:337–343. doi:10.1080/10611860500286239

Hyeon T, Lee SS, Park J, Chung Y, Na HB (2001) Synthesis of highly crystalline and monodisperse maghemite nanocrystallites without a size-selection process. J Am Chem Soc 123:12798–12801. doi:10.1021/ja016812s

Iakoubov LZ, Torchilin VP (1997) A novel class of antitumor antibodies: nucleosome-restricted antinuclear autoantibodies

(ANA) from healthy aged nonautoimmune mice. Oncol Res 9:439–446

Iakoubov LZ, Torchilin VP (1998) Nucleosome-releasing treatment makes surviving tumor cells better targets for nucleosome-specific anticancer antibodies. Cancer Detect Prev 22:470–475. doi:10.1046/j.1525-1500.1998.00055.x

Iakoubov L, Rokhlin O, Torchilin V (1995) Anti-nuclear autoantibodies of the aged reactive against the surface of tumor but not normal cells. Immunol Lett 47:147–149. doi:10.1016/0165-2478(95)00066-E

Ito A, Shinkai M, Honda H, Kobayashi T (2005) Medical application of functionalized magnetic nanoparticles. J Biosci Bioeng 100:1–11. doi:10.1263/jbb.100.1

Ito A, Honda H, Kobayashi T (2006) Cancer immunotherapy based on intracellular hyperthermia using magnetite nanoparticles: a novel concept of "heat-controlled necrosis" with heat shock protein expression. Cancer Immunol Immunother 55:320–328. doi:10.1007/s00262-005-0049-y

Jin H, Hong B, Kakar SS, Kang KA (2008) Tumor-specific nano-entities for optical detection and hyperthermic treatment of breast cancer. Adv Exp Med Biol 614:275–284. doi:10.1007/978-0-387-74911-2_31

Johannsen M, Thiesen B, Gneveckow U, Taymoorian K, Waldofner N, Scholz R, Deger S, Jung K, Loening SA, Jordan A (2006) Thermotherapy using magnetic nanoparticles combined with external radiation in an orthotopic rat model of prostate cancer. Prostate 66:97–104. doi:10.1002/pros.20324

Kang HW, Josephson L, Petrovsky A, Weissleder R, Bogdanov A Jr (2002) Magnetic resonance imaging of inducible E-selectin expression in human endothelial cell culture. Bioconjug Chem 13:122–127. doi:10.1021/bc0155521

Kubo T, Sugita T, Shimose S, Nitta Y, Ikuta Y, Murakami T (2001) Targeted systemic chemotherapy using magnetic liposomes with incorporated adriamycin for osteosarcoma in hamsters. Int J Oncol 18:121–125

Lukyanov AN, Elbayoumi TA, Chakilam AR, Torchilin VP (2004) Tumor-targeted liposomes: doxorubicin-loaded long-circulating liposomes modified with anti-cancer antibody. J Control Release 100:135–144. doi:10.1016/j.jconrel.2004.08.007

Martina MS, Fortin JP, Fournier L, Menager C, Gazeau F, Clement O, Lesieur S (2007) Magnetic targeting of rhodamine-labeled superparamagnetic liposomes to solid tumors: in vivo tracking by fibered confocal fluorescence microscopy. Mol Imaging 6:140–146

Mathieu JB, Martel S (2007) Magnetic microparticle steering within the constraints of an MRI system: proof of concept of a novel targeting approach. Biomed Microdevices 9:801–808. doi:10.1007/s10544-007-9092-0

Mulder WJ, Griffioen AW, Strijkers GJ, Cormode DP, Nicolay K, Fayad ZA (2007) Magnetic and fluorescent nanoparticles for multimodality imaging. Nanomedicine 2:307–324. doi:10.2217/17435889.2.3.307

Munshi N, De TK, Maitra A (1997) Size modulation of polymeric nanoparticles under controlled dynamics of microemulsion droplets. J Colloid Interface Sci 190:387–391. doi:10.1006/jcis.1997.4889

Nasongkla N, Bey E, Ren J, Ai H, Khemtong C, Guthi JS, Chin SF, Sherry AD, Boothman DA, Gao J (2006) Multifunctional polymeric micelles as cancer-targeted, MRI-ultrasensitive drug delivery systems. Nano Lett 6:2427–2430. doi:10.1021/nl061412u

Sawant RR, Sawant RM, Torchilin VP (2008) Mixed PEG–PE/vitamin E tumor-targeted immunomicelles as carriers for poorly soluble anti-cancer drugs: improved drug solubilization and enhanced in vitro cytotoxicity. Eur J Pharm Biopharm 70:51–57. doi:10.1016/j.ejpb.2008.04.016

Silva AK, Silva EL, Carrico AS, Egito ES (2007) Magnetic carriers: a promising device for targeting drugs into the human body. Curr Pharm Des 13:1179–1185. doi:10.2174/138161207780618993

Sun C, Veiseh O, Gunn J, Fang C, Hansen S, Lee D, Sze R, Ellenbogen RG, Olson J, Zhang M (2008) In vivo MRI detection of gliomas by chlorotoxin-conjugated superparamagnetic nanoprobes. Small 4:372–379. doi:10.1002/smll.200700784

Sykova E, Jendelova P (2007) In vivo tracking of stem cells in brain and spinal cord injury. Prog Brain Res 161:367–383. doi:10.1016/S0079-6123(06)61026-1

Tang T, Zheng JW, Chen B, Li H, Li X, Xue KY, Ai X, Zou SQ (2007) Effects of targeting magnetic drug nanoparticles on human cholangiocarcinoma xenografts in nude mice. Hepatobiliary Pancreat Dis Int 6:303–307

Torchilin VP (2004) Targeted polymeric micelles for delivery of poorly soluble drugs. Cell Mol Life Sci 61:2549–2559. doi:10.1007/s00018-004-4153-5

Torchilin VP, Levchenko TS, Lukyanov AN, Khaw BA, Klibanov AL, Rammohan R, Samokhin GP, Whiteman KR (2001) p-Nitrophenylcarbonyl-PEG–PE-liposomes: fast and simple attachment of specific ligands, including monoclonal antibodies, to distal ends of PEG chains via p-nitrophenylcarbonyl groups. Biochim Biophys Acta 1511:397–411. doi:10.1016/S0005-2728(01)00165-7

Torchilin VP, Lukyanov AN, Gao Z, Papahadjopoulos-Sternberg B (2003) Immunomicelles: targeted pharmaceutical carriers for poorly soluble drugs. Proc Natl Acad Sci USA 100:6039–6044. doi:10.1073/pnas.0931428100

Wada S, Tazawa K, Furuta I, Nagae H (2003) Antitumor effect of new local hyperthermia using dextran magnetite complex in hamster tongue carcinoma. Oral Dis 9:218–223. doi:10.1034/j.1601-0825.2003.02839.x

Yang F, de Fu L, Long J, Ni QX (2008) Magnetic lymphatic targeting drug delivery system using carbon nanotubes. Med Hypotheses 70:765–767. doi:10.1016/j.mehy.2007.07.045

Zhang C, Jugold M, Woenne EC, Lammers T, Morgenstern B, Mueller MM, Zentgraf H, Bock M, Eisenhut M, Semmler W, Kiessling F (2007) Specific targeting of tumor angiogenesis by RGD-conjugated ultrasmall superparamagnetic iron oxide particles using a clinical 1.5-T magnetic resonance scanner. Cancer Res 67:1555–1562. doi:10.1158/0008-5472.CAN-06-1668